Engineering Honors Capstone: Manipulation of biomechanics in composite hydrogels using ultrasound to control cell behavior

Easton Farrell

Abstract

Cells respond to biochemical and biomechanical cues (e.g., stiffness) from the surrounding extracellular matrix (ECM). Cellular differentiation into more specialized cell types is a common cellular response intimately related to these cues. Regenerative medicine often employs implantable hydrogel scaffolds as surrogates of the native ECM and as carriers of biomolecules and cells. The mechanical properties of hydrogels are conventionally designed *a priori* and are often static and uniform. That is to say, the mechanical properties cannot be dynamically controlled following implantation in a user-defined, on demand manner. The Fabiilli lab utilizes specialized composite hydrogel scaffolds that have mechanical characteristics that can be modulated when focused ultrasound (FUS) is applied. These scaffolds, termed acoustically-responsive scaffolds (ARSs), consist of a phase-shift emulsions (PSE) embedded within a polymerized fibrin matrix. PSE is non-thermally vaporized when FUS is applied, and expands into a gas bubble, thereby causing localized compaction and significant increases in stiffness of the matrix surrounding the bubble.[1] In this *in vitro* study, we investigate how these localized increases in matrix stiffness can be used to control the differentiation of fibroblasts into myofibroblasts, a transition which occurs at high stiffnesses.[2] Findings indicated that vaporized PSE generated stable bubbles as well as bubbles that recondensed within the ARS, and that αSMA intensity was qualitatively higher at locations proximal to vaporized PSE compared to distal locations. Quantitatively, the normalized aSMA signal intensity was significantly increased in regions proximal to the vaporized PSE ($p = 0.0007$ and $p = 0.0478$).

1 INTRODUCTION

Cells in the body respond to chemical and biomechanical cues from their local environment. Cell behavior is modulated in response to these signals, facilitated by a cascade of chemical reactions engendered within the cell that eventually instigate the behavioral change. Amongst the behaviors affected by these cues is the differentiation of cells into new fates and specialized cell types. This behavior can be controlled to some degree with laboratory protocols involving manufactured cell microenvironments composed of specific chemical combinations and mechanical properties that provoke differentiation into desirable fates. For instance, protocols have been developed to differentiate pluripotent stem cells – cells with high potential to differentiate into other cell types – into vascularized cerebral organoids.[3,4]

Fibroblast progression into a myofibroblast fate is another such differentiation that can be enhanced by properties of experimentally-controlled microenvironments. Previous research has demonstrated that fibroblast differentiation into myofibroblasts can be induced by culturing the cells in high-stiffness environments. According to Huang and colleagues,[2] mean stiffnesses of approximately 20 kPa were sufficient to significantly enhance differentiation into myofibroblast fates, as supported by an increase in alpha smooth muscle actin (αSMA) signal.

Research on controlling differentiation into myofibroblast fate is therapeutically relevant, since myofibroblasts are critical in the wound repair process. They generate and orchestrate the placement of extracellular matrix and are thus pivotal in wound closure.[5,6] However, over-active and under-regulated myofibroblast activity has been connected to contracture, fibrotic scarring, and organ dysfunction. Research that aims to tightly regulate myofibroblast activity in a way supportive of wound healing yet mitigative of these disorders is therefore a valuable endeavor.

A common strategy employed in regenerative medicine is the use of implantable hydrogel matrices as surrogates for the native ECM. These hydrogels can be used as compartments for cells, or they can be utilized for delivery of regenerative biomolecules. The Fabiilli lab has developed specialized composite fibrin hydrogels called acoustically-responsive scaffolds (ARSs), which have the added quality of being responsive to focused ultrasound exposure (FUS), thereby enabling control of the hydrogel's properties in both space and time. For example, ultrasound can be used to control the release of growth factors encapsulated within double emulsion droplets that are embedded within the ARS. Ultrasound causes a phase within the phase-shift emulsion (i.e., perfluorocarbon) to vaporize, thereby disrupting the particle morphology. Before the ratification of my Capstone proposal, the lab had primarily explored the use of ARSs for the delivery of biochemical signaling molecules *in vivo* (e.g., growth factors) to stimulate processes such as angiogenesis. However, there was a need to better elucidate how biomechanical signals such as matrix stiffness and elasticity could be spatiotemporally controlled with our method, and to demonstrate how this method could affect cellular behaviors critical for regeneration. Specifically in reference to myofibroblast differentiation, which necessitates tight control *in situ,* the highly dynamic and controllable nature of the ARSs lends credibility to a project exploring their ability to promote the behavior.

The project focuses on non-invasively controlling biophysical properties of the ARS using ultrasound in an effort to control cellular behavior. As demonstrated by our preliminary data, ultrasound can induce localized matrix compaction and stiffening within fibrin-based ARSs (see Figure 1). The goal of this capstone project was to use these ultrasound-induced changes to control the differentiation of fibroblasts into myofibroblasts, a process that is mediated by matrix stiffness. The study examined how different properties of the ARS (e.g., emulsion type) and ultrasound impact differentiation induced by biomechanical changes. Findings from this study would provide a proof-of-concept that ultrasound can induce biomechanical changes in a hydrogel that impact cell differentiation in a way that credibilizes a viable therapeutic method.

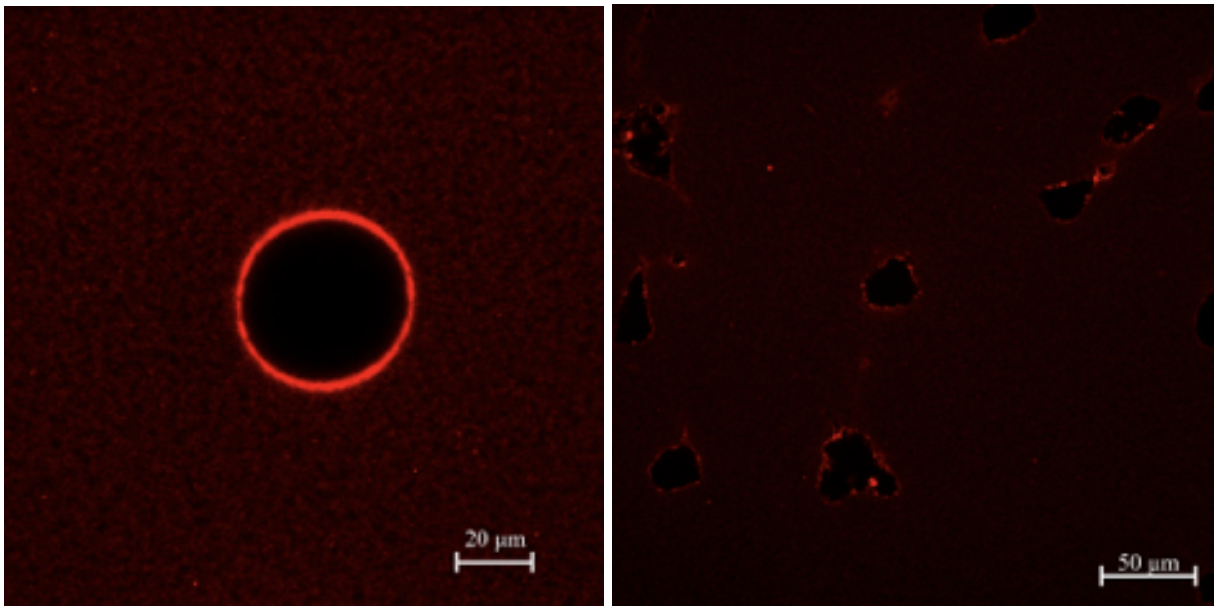

Figure 1. Confocal images taken of stable bubbles (left) and recondensed bubbles (right) that were generated by FUS application to ARSs. Brighter areas indicate that the stiffness is higher due to local matrix compaction caused by the bubble events. This finding was an influence on this project, which sought to utilize the transmutability of the matrix to induce a cellular response.

The capstone study aimed to address the following questions:

Is our vaporized emulsion bubble method able to be used to influence cellular behavior? Can we demonstrate this by inducing differentiation of fibroblasts into myofibroblasts? A significant increase in myofibroblast differentiation experienced by cells proximal to the stable or recondensed bubbles would support this claim by demonstrating colocalization of myofibroblast fate with increased stiffness due to matrix compaction.

Are there other controllable factors that could enhance or otherwise influence the extent of differentiation (e.g., fibrin density, type of perfluorocarbon)? It is possible that even if the bubble events do increase the stiffness of the gel locally, the starting gel is not dense enough for this effect to raise stiffness to a sufficient level to induce differentiation. It is also possible that, given the different properties of various perfluorocarbons (e.g., vaporization temperature, stability of progeny bubbles, etc.), some perfluorocarbons would be more or less successful than others at producing a modulatory effect.

How close do the cells need to be to the bubble event in order for the effect to be noticeable? Also, since the bubbles do not instantaneously expand to their stable size, is there a specific time following ultrasound exposure needed for the effect to be seen?

2 METHODS

Micron-sized PSE containing perfluorohexane (C_6F_{14}) was produced using a microfluidic chip and incorporated into cylindrical ARSs. For experiment 3 (described below in section 2.3), PSE containing perfluoroheptane (C_7F_{16}) was produced and utilized in the same manner.

This project was carried out in three separate experiments. An inaugural experiment evaluated perfluorohexane (C6) as the agent contained within the emulsions, the second controlled for a possible factor perniciously contributing to differentiation, and the third studied perfluoroheptane (C7) as the emulsion-embedded agent.

2.1 Experiment 1: Development of ARSs with C6 emulsions, no buffer period

Several sets of 500 microliter ARSs were constructed (5 mg/mL fibrin, 0.01% (v/v) perfluorohexane phase shift emulsion (PSE), 2 U/mL thrombin) and exposed to focused ultrasound (2.55 MHz, f-number: 0.83, 6 MPa peak rarefactional pressure, 5.4 microsecond pulse duration, 100 Hz pulse repetition frequency). The ARSs were manufactured in 24-well BioFlex ® plates. Following the focused ultrasound exposure, normal human dermal fibroblasts (NHDFs) were plated on top of the ARSs at 2600 cells/cm^2. Figure 2 schematitizes the setup of the gels and added cells. The ARSs were then incubated at 37 ℃ and 5% CO_2 for 2 days before being stained for the myofibroblast marker alpha-smooth muscle actin (αSMA). Cells were counterstained with the actin filament marker phalloidin and Hoescht nuclear dye.

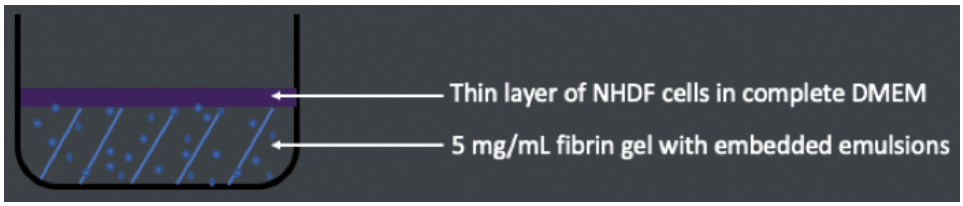

Figure 2. Fibrin hydrogels were constructed with embedded phase-shift emulsions containing perfluorocarbons, as represented by the speckled patterning in the above depiction. NHDF cells were plated atop the gels in a suspension of complete DMEM. After a short time, these cells settled to the top of the gel where they could interact with the expanding emulsion bubbles.

2.2 Experiment 2: Development of ARSs with C6 emulsions, with 2-day buffer period

Since fibroblast differentiation into a myofibroblast fate can be induced via high stiffnesses, it is possible that the maintenance of the NHDF cells on hard-bottomed Corning Cell Culture Plates could influence this fate before the experiment was enacted. Therefore, in order to control for this possibility, NHDF cells were layered atop the ARSs before the focused ultrasound exposure

was applied. ARSs with layered cells were incubated at 37 ℃ and 5% CO_2 for two days before ultrasound exposure, influencing the cells back to a fibroblasts fate by virtue of the less-stiff matrix environment. All other considerations, gel characteristics, and ultrasound characteristics were maintained.

2.3 Experiment 3: Development of ARSs with C7 emulsions, with 2-day buffer period

When the second experiment was run, we noted that spontaneous vaporization of some of the C6 emulsions was engendered by the 2-day incubation period before FUS exposure, likely attributable to the incubator achieving a sufficiently high temperature to cause vaporization. Perfluoroheptane (C7) has a higher vaporization temperature than C6 (82.5 ℃, as compared to 56 ℃), suggesting that the spontaneous vaporization during the incubation period would not be as likely with the new perfluorocarbons. Therefore, a set of ARSs containing C7 emulsion instead of C6 emulsion were developed, incubated, exposed to ultrasound, and stained for αSMA, phalloidin, and Hoescht nuclear stain.

2.4 Cell staining protocol

The following staining protocol was performed with no variations on all of the scaffolds from each of the experiments.

Following the two day period after FUS exposure, overlying media was removed from the scaffolds, and 1 mL of Z-Fix was added to fix the cells. After a 20 minute incubation, the Z-Fix was removed and washed in a triplicate of 5 minute PBS applications while on an orbital shaker (100 rotations/min). 1 mL of Triton X-100 was then added atop each scaffold in order to permeabilize the membranes in preparation for the stains. After another 20 minute incubation and triplicate wash, blocking buffer was added (1 mL/scaffold) and left for 1 hour at room temperature. This was done in order to mitigate propensity for off-target binding. Following this, another triplicate wash preceded application of the antibodies anti-αSMA and phalloidin (200 microliters per scaffold, 0.25% (v/v) anti-αSMA and 0.25% (v/v) phalloidin in PBS).

The anti-αSMA antibody and the phalloidin were conjugated with Alexa Fluor 555 and Alexa Fluor 488, respectively, so a separate secondary staining was not necessary.

After an overnight incubation with the antibody, the overlying media was removed and the scaffolds were washed in triplicate before each receiving 1 mL of 0.01% (v/v) Hoescht dye in PBS to stain the cell nuclei. After another overnight incubation and a triplicate wash, the scaffolds were prepared for immunofluorescence imaging.

2.5 Imaging of stained scaffolds

Images of αSMA signal were taken at 1 s exposure time with the Cy5 channel. Phalloidin images were taken at 300 ms exposure time with the GFP channel. DAPI images were obtained under 50 ms exposure time, and brightfield images were taken under 60 ms exposure time.

Four images – one each for αSMA, phalloidin, DAPI, and brightfield – were taken at locations where bubble events interacted with cells. Phalloidin staining was primarily used to indicate the presence of fibroblasts as denoted by actin filaments. Brightfield images were used for orientation and to better understand the bubble events being observed. DAPI and αSMA stains were used for quantitative analysis as described below.

2.6 Analysis of images

A defensible metric for degree of myofibroblast activity is intensity of the αSMA signal expressed by the cells. The goal of the project was thus to demonstrate that cells at the immediate peripheries of bubble events (which are known to introduce local compaction of matrix and thus generate increased stiffness) reported higher average αSMA signal than cells distal from the bubble events. Representative proximal and distal regions of interest in an αSMA image are provided in Figure 3.

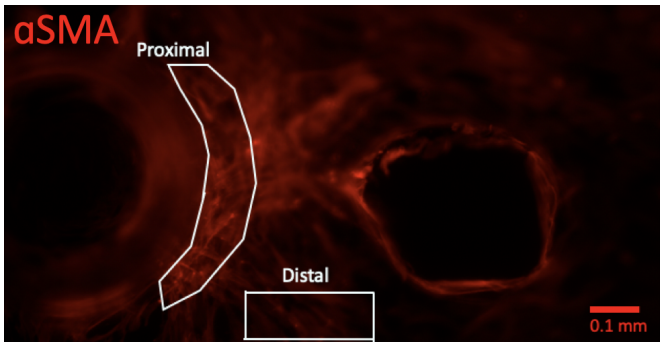

Figure 3. Typical proximal and distal regions of interest identified for quantitative analysis of αSMA signal intensity. Proximal measurements were kept within about 20 pixels (~0.075 mm) of the stable or recondensed bubble's edge. A definitive "halo-effect" of the αSMA signal (as shown above) was observed around a large percentage of the bubble events.

In order to quantify the average αSMA intensity per cell, ImageJ software was used to draw regions of interest proximal to the bubble peripheries and distal from the bubble events. Using the measuring tool, average pixel intensity was calculated for these regions. Next, equivalent regions of interest were copied onto the affiliated DAPI images, and the number of cells per

region of interest was counted. The αSMA intensity value was then divided by the number of cells to generate values for the average αSMA intensity per cell in distal and proximal regions.

3 RESULTS

A 2-day incubation period following the FUS exposure proved to be an appropriate time for the bubbles to expand and for the cells to differentiate. This timing was predicted based on the experimental setup of Huang and colleagues – which demonstrated that a period of only 24-48 hours was necessary for fibroblasts to be under high-stiffness conditions before differentiation – and confirmed by the results we observed in the first iteration of the experiment.

A representative quadruplet of images obtained from this project is provided in Figure 4, alongside a merged image of the αSMA, phalloidin, and DAPI stains, and a line plot of pixel intensity. Images such as those provided in the figure demonstrate the localized enhancement of αSMA intensity in areas close to the peripheries of stable and recondensed bubbles. This qualitative relationship demonstrates a proof-of-concept that FUS can be applied to our ARSs for the use of influencing fibroblast differentiation.

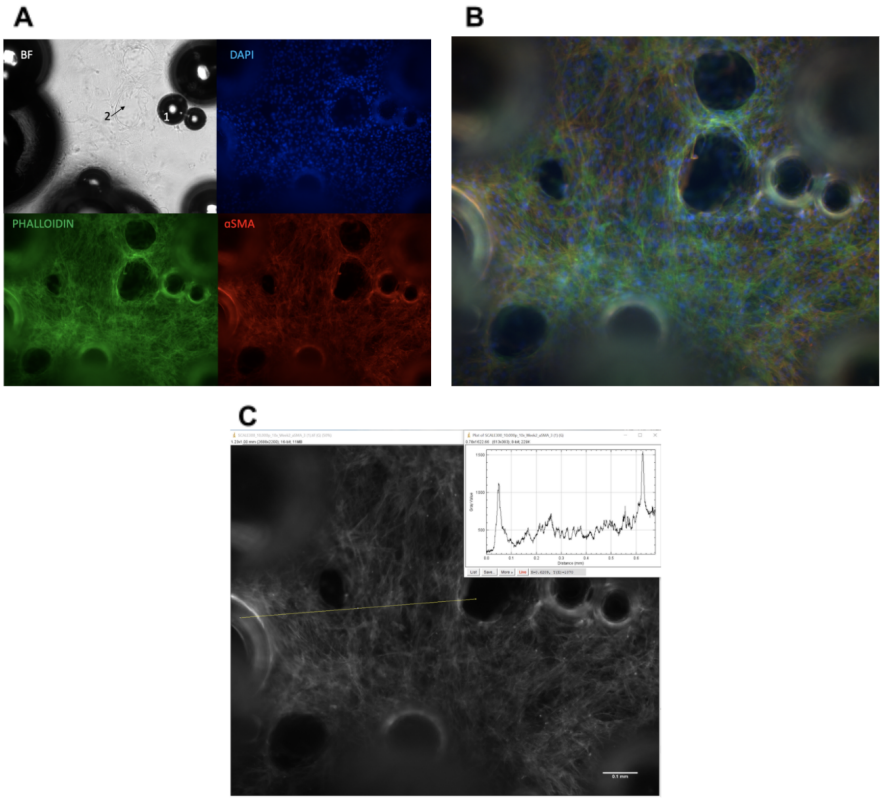

Figure 4. Representative quadruplet of images obtained from the experiments, showing brightfield, DAPI, phalloidin, and αSMA images of the same area of interest (A); Overlay image of the phalloidin,

αSMA, and DAPI stains demonstrates brighter αSMA and phalloidin signalling around bubble event peripheries (B); Average αSMA intensity reported as a line plot of the yellow line in the image, which passes through a recondensed bubble (correlated to the first peak in intensity), and a stable bubble (second peak).

In the first experiment, average intensity for αSMA signal was significantly greater for cells proximal to bubble events than for cells distal from events (two-tailed, unpaired t-test with Welch's correction, $p = 0.0007$). This difference was also upheld in the second experiment in which cells were given a 2-day incubation period atop the gels before ultrasound exposure, though to a lesser degree of significance ($p = 0.0478$). Finally, there was also a significant enhancement in myofibroblast fate for the fibroblasts atop the C7-loaded ARSs when comparing proximal to distal cells ($p = 0.0006$). This data is summarized in Figure 5.

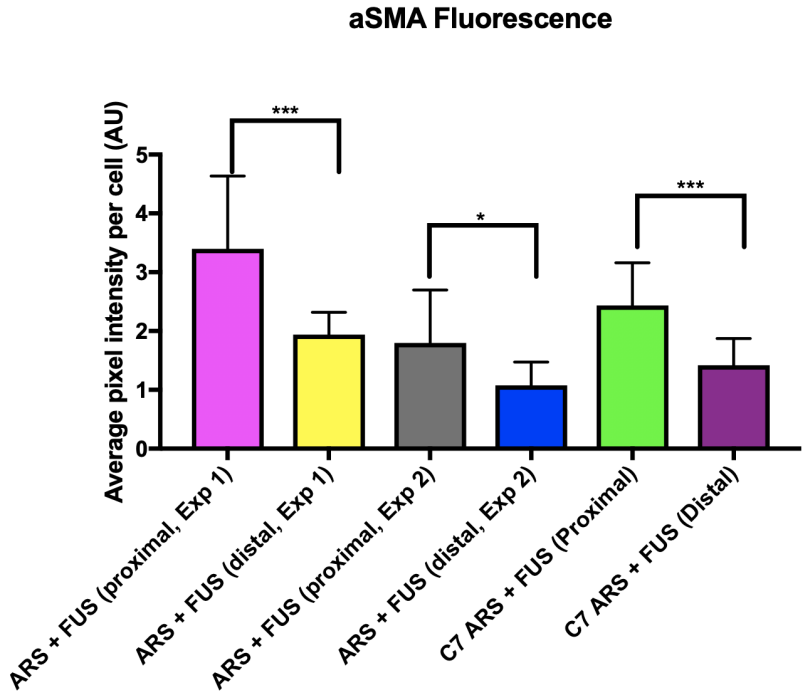

Figure 5. In each of the three experiments, cells proximal to bubble events expressed significantly higher levels of the myofibroblast marker αSMA ($p = 0.0007$ for experiment 1 with C6 and no buffer period, $p = 0.0478$ for experiment 2 with C6 and a 2-day buffer period, $p = 0.0006$ for experiment 3 with C7 and a 2-day buffer period.

Proximal αSMA expressions from experiments 2 and 3, which both added the 2-day control period before ultrasound exposure to mitigate any myofibroblast differentiation before experimentation, did in fact yield decreased mean intensities when compared to the distal means ($p = 0.0018$ for C6 vs C6 with time buffer; $p = 0.0222$ for C6 vs C7 with time buffer). Additionally, no significant difference was observed between proximal cells in the C6 gels given a buffer period and the C7 gels given a buffer period ($p = 0.1027$). This information is summarized in Figure 6.

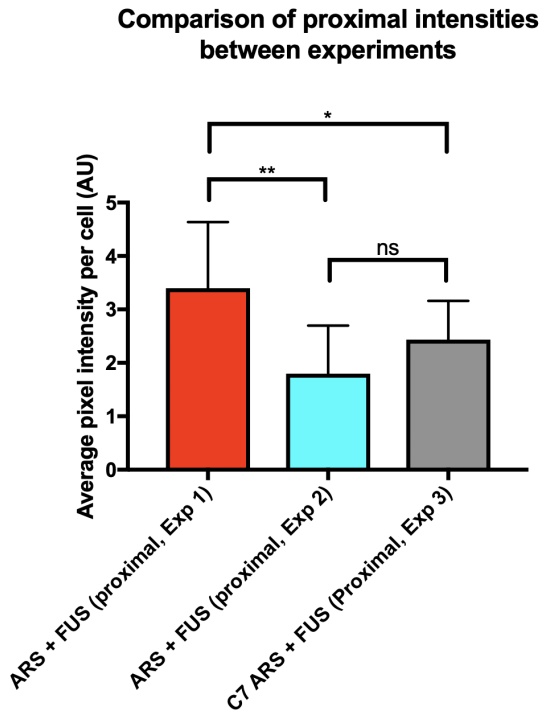

Figure 6. Introducing the 2-day buffer period between cell placement on the gel and ultrasound exposure significantly decreased the αSMA signal at the proximities of the bubble events. Although mean αSMA intensity was greater in experiment 3 in which C7 was used in replacement of C6, the difference was not significant ($p = 0.1027$).

DISCUSSION & APPLICATION

FUS-induced stiffening of the ARS caused a localized increase in aSMA intensity in NHDFs. As corroborated by the results, myofibroblast differentiation, reported by alpha smooth muscle actin signal, is enhanced near the peripheries of stable and recondensed bubbles generated by FUS application to fibrin-based ARS hydrogels. Given the similarity between the images reporting increased stiffness proximal to the bubbles (Figure 1) and the images demonstrating increased

αSMA signal at the bubble peripheries, it appears that the droplet expansion-induced local gel compaction is responsible for the increased propensity towards the myofibroblast fate. This provides a proof-of-concept for our question about the ability of mechanical gel modulation using our ARS + FUS technique to affect cellular behavior.

Although future research should be conducted to provide a more robust claim, our research indicates that a starting density of 5 mg/mL fibrin when constructing the hydrogels provides an adequate initial stiffness to support the trends we observed towards myofibroblast differentiation. Furthermore, although it is possible that an even shorter time following ultrasound may be needed for the cells to modulate their behavior, an interval of two days was demonstrated to be appropriate.

The type of perfluorocarbon (perfluorohexane or perfluoroheptane) used did not have a significant impact on the cells, despite their variations in bubble stability, size, and vaporization temperatures. Conversely, allowing for a 2-day buffer period after plating the cells but before applying FUS did significantly impact the results. It is possible that reiterations of the experiment allowing for larger buffer periods may further decrease the mean average αSMA intensity. However, based on the significant differences between the proximal and distal cells for these gels in spite of decreased mean intensity, we do not believe that this constitutes a strong argument against our technique. Nonetheless, steps will be taken in the future to ensure the results are as expected for longer buffer periods.

Future research will involve qPCR analysis of gels given our treatment to evaluate the extent to which the mRNA sequence responsible for αSMA activity is expressed. An outcome from this analysis that demonstrates increased mRNA activity amongst cells from bubble-containing ARSs would further corroborate our bed of evidence.

This project lends credibility to an *in vivo* study that implants the ARSs alongside host-derived fibroblasts in an effort to enhance wound repair for internal injuries like lesions or blood vessel hemorrhages. Although the vision of how our findings could be applied for a therapeutic option is somewhat nebulous since the findings are novel, there is merit to exploring such options. Patients on blood thinners may benefit greatly from an implantable device capable of mitigating excess bleeding in especially worrisome areas (e.g., at locations of port insertions for breast cancer patients). Patients undergoing invasive surgeries may benefit from the implant, as well, due to its implied ability to controllably bolster the wound repair process.

Furthermore, this project's findings should inspire more research of the ARSs' ability to stimulate differentiation or other favorable behaviors of more cells besides fibroblasts. One commonly-sought finding is a method that can controllably influence mesenchymal cells towards an articular cartilage or bone-remodeling cell fate. Since cartilage and bone tissue is keenly responsive to mechanical cues (e.g., weight loading, substrate stiffness, etc.),[7,8] it is pertinent to explore application of the FUS-induced stiffening of the hydrogels to embedded mechanical stem

cells. Establishing the ability to exert spatiotemporal control on mesenchymal stem cell differentiation would constitute a significant therapeutic breakthrough.

Future studies will continue to investigate how FUS-induced modulation of the mechanical properties of ARSs can be used in the study of mechanobiology. Using the results of this capstone as a guide and proof-of-concept, the lab will continue to explore applications of their novel hydrogels.

CITATIONS

[1] Aliabouzar, Mitra, Davidson, Christopher D, Wang, William Y, Kripfgans, Oliver D, Franceschi, Renny T, Putnam, Andrew J, Fowlkes, J. Brian, et al. (2020). Spatiotemporal control of micromechanics and microstructure in acoustically-responsive scaffolds using acoustic droplet vaporization. See DOI: 10.1039/d0sm00753f. Soft matter, 16(28), 651–6513.

[2] Huang, Xiangwei, Yang, Naiheng, Fiore, Vincent F, Barker, Thomas H, Sun, Yi, Morris, Stephan W, Ding, Qiang, et al. (2012). Matrix Stiffness–Induced Myofibroblast Differentiation Is Mediated by Intrinsic Mechanotransduction. *American journal of respiratory cell and molecular biology*, *47*(3), 340–348. Article, NEW YORK: American Thoracic Society.

[3] Lancaster, Madeline A, & Knoblich, Juergen A. (2014). Generation of cerebral organoids from human pluripotent stem cells. *Nature protocols*, *9*(10), 2329–2340. Research Support, Non-U.S. Gov't, England: Springer Science and Business Media LLC.

[4] Ham, Onju, Jin, Yeung Bae, Kim, Janghwan, & Lee, Mi-Ok. (1/1/2020). Blood vessel formation in cerebral organoids formed from human embryonic stem cells. Biochemical and Biophysical Research Communications, 521(1), 84–90. Journal Article, United States: Elsevier Inc.

[5] Chitturi, Ravi Teja, Balasubramaniam, A Murali, Parameswar, R Arjun, Kesavan, G, Haris, K T Muhamed, & Mohideen, Khadijah. (2015). The role of myofibroblasts in wound healing, contraction and its clinical implications in cleft palate repair. Journal of international oral health, 7(3), 75–80. Journal Article, India: Medknow Publications & Media Pvt. Ltd.

[6] Hinz, B. (2016). The role of myofibroblasts in wound healing. Current research in translational medicine, 64(4), 171–177. Research Support, Non-U.S. Gov't, France: Elsevier BV.

[7] Cai, Linyi, Liu, Wenjing, Cui, Yujia, Liu, Yang, Du, Wei, Zheng, Liwei, Pi, Caixia, et al. (2020). Biomaterial Stiffness Guides Cross-talk between Chondrocytes: Implications for a Novel Cellular Response in Cartilage Tissue Engineering. ACS biomaterials science & engineering, 6(8), 4476–4489. American Chemical Society.

[8] Heath, Carole A. (2000). The Effects of Physical Forces on Cartilage Tissue Engineering. Biotechnology & genetic engineering reviews, 17(1), 533–552. PART 7 Polysaccharide Biotechnology, England: Taylor & Francis Group.